RSC Advances

ROYAL SOCIETY OF CHEMISTRY

www.rsc.org/advances

Comparison of degradation features of lignin to phenols over Pt catalysts prepared with various forms of carbon supports

Jeesu Park[a], Shinyoung Oh[a], Jae-Young Kim[a], Shin young Park[a], In Kyu Song[b], Joon Weon Choi[c*]

[a] Department of Forest Sciences, College of Agricultural and Life Science, Seoul National University, 599 Gwanak-ro, Gwanak-gu, Seoul, 151-921, Republic of Korea

[b] School of Chemical and Biological Engineering, Institute of Chemical Processes, Seoul National University, 599 Gwanak-ro, Gwanak-gu, Seoul, 151-921, Korea

[c] Graduate School of International Agricultural Technology and Institute of Green-Bio Science and Technology, Seoul National University, Pyeongchang 232-916, Republic of Korea

* Corresponding author. Tel: +82-33-339-5840; Fax: +82-33-339-5689
E-mail address: cjw@snu.ac.kr

Abstract

Soda lignin separated from wheat straw was successfully depolymerized to produce the phenol-rich oil fraction over various carbon-supported platinum (Pt) catalysts. Three different supports (mesoporous carbon (STC), porous carbon (TC), and microporous carbon (DC)) were prepared; 5 wt% Pt on commercial activated carbon (Pt/C) was also used as a comparison. The surface characterizations of catalysts were examined by FE-SEM, BET, XRD, XPS and HR-TEM. The Pt/C and Pt/STC proved to be superior catalysts for producing high yields of lignin-oil (Pt/C: 79.9 wt% and Pt/STC: 79.4 wt%) with low amounts of char (Pt/C: 4.2 wt% and Pt/STC: 7.6 wt%) compared to the other catalysts. This is due to the fine dispersion of Pt (i.e., higher BET surface area) on these carbon supports. In addition, we found a high correlation between the BET surface area (Pt dispersion) and the molecular weight of the lignin-oil. The amounts of monomeric phenol compounds, which are mainly composed of 4-ethlyphenol, 4-methylguaiacol, and 4-propylguaiacol, were also higher with Pt/C (90.92 mg/g of lignin) and Pt/STC (78.06 mg/g of lignin) compared to the other samples.

Keywords: Lignin depolymerization, supercritical ethanol, supported carbon, platinum catalyst, phenols

1. Introductions

Lignin is a three-dimensional amorphous phenolic polymer that accounts for 10-30 wt% of lignocellulosic biomass. This structural component of biomass is comprised of three kinds of lignin monomers (phenylpropane unit: C3C6), including *p*-coumaryl, coniferyl, and sinapyl alcohol with various inter-unit linkages such as β-O-4 (40-60%), α-O-4 (3-5%), biphenyl (3.5-25%), and β-5 (4-10%) [1]. Recently, interest in lignin utilization as a value-added source has increased because over 50 million tons of lignin byproducts are generated annually by the US pulping/paper industry. Moreover, a great deal of research has been carried out on the biochemical conversion of lignocellulosic biomass to biosugar or bioethanol, which also generates lignin byproducts in the pretreatment and hydrolysis steps [2]. However, only 2% of lignin byproducts from these processes are converted into value-added products, while the rest are combusted for heat generation in industrial plants [3].

Lignin is a high molecular weight polymer composed of alkyl phenol unites [4]. Therefore, it can be regarded as a rich source of phenols, which are widely used for the replacement of chemical intermediates that have historically been synthesized from petrochemical resources [5]. However, it is difficult to decompose lignin into monomeric phenols because of its complex structure [6]. Catalytic degradation is a very promising process for the conversion of the complex lignin compound into small molecules for fuels and basic chemicals or oligomers for further applications; this can generate value-added products from lignin raw materials [7]. Some work has already been done using noble metal catalysts because they are known to be active with respect to hydrogenation and hydro-deoxygenation [8]. For example, switch grass lignin was converted into monomeric phenols over a noble metal catalyst (Pt) with formic acid as the hydrogen donor; this resulted in a significant reduction in the molecular weight and oxygen content of the lignin [9]. Yan et al. also reported that noble metal catalysts have

shown excellent chemo-selectivity for aromatic products as well as high activity for C-O bond cleavage [10]. Additionally, Kim et al. have shown that Pt/C was the most effective catalyst in the lignin depolymerization process (among Pd/C, Ru/C, and Ni/C catalysts) for producing large amounts of lignin-oil (77.4 wt%) with the smallest amount of char (3.7 wt%) as well as the highest selectivity for 4-ethylphenol, guaiacol, 4-ethylguaiacol, and syringol [11].

However, noble metal catalysts are expensive; to solve this problem, supporting materials are used for metal dispersion and for controlling the size of the metal clusters. A major role of the support material is to stabilize the active catalytic species in a highly dispersed form. Therefore, much of the research focusing on Pt catalysts has focused on finding efficient supporting materials. For example, recently, a number of other studies provided Pt catalyst supported on N-containing carbon and proved it is superior over normal Pt/C [12-15]. Likewise, carbon materials have been reported to be one of the most efficient supports due to their excellent thermal and mechanical stability [16]. In particular, carbon synthesized with uniform mesopores has shown great potential as a supporting material because of its large surface area and pore volume [17]. Carbon can act as an excellent support for Pt if it is fabricated such that it has a controllable pore structure for increasing the catalyst dispersion, which will be effective for lignin deploymerization and allow for hydrogenation and hydro-deoxygenation [18]. However, the effect of the supporting material on lignin depolymerization has yet to be studied.

Therefore, in this study, carbon-based supporting materials were prepared through various methods [18(a)]. These were characterized by BET, FE-SEM, XRD, XPS and HR-TEM. Lignin depolymerization was carried out over four different Pt catalysts under supercritical ethanol, which has high heat transfer, high dispersion capacity, high lignin solubility, and hydrogen donor capacity [11]. The depolymerized lignin product (lignin-oil) was then analyzed in terms of its physicochemical properties by GPC, elemental analysis, and GC/MS in order

to compare the catalytic activities of the supporting materials on lignin depolymerization.

2. Experimental

2.1 Lignin sample

Soda lignin (Protobind 1000), which was used as the raw material in this study, was generated through a soda process from herbaceous crops of wheat straw and sarkanda grass that were purchased from Granit Research and Development SA.

2.2 Preparation of carbon-supported Pt catalysts

Schematic procedures for the production of various carbon supports are shown in Figure 1 [18(a)]. In this study, Pt supported on an activated carbon catalyst (Pt/C) was purchased from Sigma-Aldrich (CAS No. 7440-06-4); this was used without further treatment. For comparison, mesoporous carbon (STC), porous carbon (TC), and microporous carbon (DC) supports were prepared by a surfactant-templating method, templating method, and direct carbonization method, respectively. Preparation of Pt catalysts supported on carbon supports (Pt/STC, Pt/TC, and Pt/DC) was then conducted by an incipient wetness impregnation method. Pt loading was fixed at 5 wt% in all of the catalysts. The detailed preparation procedures for these catalysts can be found elsewhere [18(a)].

2.3 Catalyst characterization

Surface areas and pore volumes of the support catalysts were calculated using BET equations and the BJH model, respectively. The structure and morphologies were examined by FE-SEM (Carl Zeiss- SUPRA 55VP). The crystalline states and particle sizes of the Pt on the supported catalysts (Pt/C, Pt/DC, Pt/TC, and Pt/STC) were characterized via X-ray powder diffraction (XRD) equipped with a Bruker D8 Advance instrument using Cu-Kα

radiation (λ = 1.541 Å) operated at 50 kV and 100 mA. Surface characterization of the Pt has been carried out by AXIS-HSI (Kratos Inc.) X-ray photoelectron spectroscopy (XPS) using a monochromatic Al Kα source (18mA, 12kV). Spectra were analyzed using CasaXPS software. Pt dispersion on the supports was examined by HR-TEM (Carl Zeiss- LIBRA120).

2.4 Depolymerization of lignin to lignin-oil over various carbon-supported Pt catalysts

All lignin depolymerization processes were operated by a three-port Parr instrumental reactor (stainless steel (SUS316); 60 mm in length, 35 mm in diameter, and a wall thickness of 30 mm). The reactor includes a heater that can heat up to 400 °C. It also has a maximum pressure of 20 MPa and a volume of 40 ml. For each reaction, 0.5 ± 0.01 g of soda lignin and 20 ml of ethanol (EtOH, ACS grade, ≥99.5%, Sigma-Aldrich) were added to the reactor with 0.025 g of 5 wt% platinum catalyst supported on carbon (Pt/C, Pt/DC, Pt/TC, and Pt/STC). The reactor was then completely sealed and sufficient nitrogen gas (99.9 %) was slowly flowed into the reactor to remove any unnecessary reactive gases. Additionally, 3 MPa of hydrogen (99.9 %) was injected into the sealed reactor before the start of the reaction. Once the three-port of reactor was inserted into the heated furnace, a 300 rpm mechanical stirrer was used to stir the lignin, ethanol, and catalyst mixture. Lignin depolymerization was carried out at 350 °C for 40 min, which conditions brought the highest yield of depolymerized lignin oil among various reaction conditions (details are shown in Table S1). The average heating rate up to 350 °C was 14.6 °C/min and the average cooling rate (to below 100 °C) was -33.4 °C/min. The recoverable products (lignin-oil, char, and gas) obtained from the reaction were separated by Kim's method [19]. The yields of the main products were calculated as follows:

(1) Lignin-oil yield (wt%)

= [weight of oil fraction (g)/ weight of lignin (g)] × 100

(2) Char yield (wt%)

= [(weight of solid fraction (g) − weight of catalyst (g))/ weight of lignin (g)] × 100

(3) Gas yield (wt%)

= 100 − (lignin-oil yield + char yield)

All experiments were repeated three times and the data were obtained by taking the mean values of the three trials.

2.5 Gel permeation chromatography (GPC)

A gel permeation chromatographer (GPC) was used to measure the average molecular weight distribution of the lignin-oil. Samples for analysis consisted of approximately 2 mg of lignin-oil dissolved in 2 ml of tetrahydrofuran; this solution was filtered using a 0.45 mm polytetrafluoroethylene (PTFE) filter. The GPC instrument was equipped with a three column system: PLgel 3-μm MIXED-D columns (300 × 7.5 mm, Varian, Inc.), a PLgel 3-um MIXED-E column (300 × 7.5 mm, Varian, Inc.), and a PLgel 5-μm guard column (50 × 7.5 mm, Varian, Inc.). The effluents were detected by UV-Vis detection (VE3210, Viscotek). 10 types of polystyrene (M_w: 580 to 3,250,000 Da) and styrene (M_w: 104.15) were used to create a calibration curve in order to calculate the molecular weight (M_w) of the effluent.

2.6 Elemental analysis

10 mg of the depolymerized lignin-oil was collected to determine the carbon, hydrogen, nitrogen, oxygen, and sulfur weight percentages using an elemental analyzer (US/CHNS-932, LECO Corp). The oxygen content was obtained as a difference.

2.7 Gas chromatography/mass spectroscopy (GC/MS) analysis

Lignin-oil was diluted with 5 ml of acetone (ACS grade, ≥99.5%, Sigma-Aldrich), and then 1 ml of the diluted sample was mixed with 20 µl of fluoranthene (50.5 mg/5 ml in acetone) as an internal standard (IS) for the preparation of GC/MS samples.

1.0 µl of the diluted sample was injected in a GC/MS (Agilent HP7890B) equipped with an Agilent HP5975A mass selective detector (MSD). The analytical column connected to the system was a DB-5 capillary column (30 mm × 0.25 mm ID × 0.25 µm film thicknesses) with a split ratio of 1:15. 99.9% helium was used as a carrier gas with a flow rate of 1 ml min^{-1}. The column temperature program was as follows. The initial oven temperature was 50 °C for 5 min. This was followed by an increase in temperature at a rate of 3 °C/min up to 300 °C for 10 min. The injector and detector temperatures were maintained at 220 °C and 300 °C, respectively. Each compound mass spectrum was identified using NIST MS Search 2.0 (NIST/EPA/NIH Mass Spectral Library; NIST 02). To determine the ratio between a signal produced by an analyte and the quantity of that analyte, response factors (Rf) were established with a concentration series of authentic standards: phenol, p-cresol, guaiacol, 4-ethylphenol, 4-methylguaiacol, 3-methoxycathecol, 4-ethylguaiacol, 4-vinylguaiacol, syringol, 4-propylguaiacol, 4-methylsyringol, 4-propylsyringol, and acetosyringone (Sigma-Aldrich). The analyte concentration was in turn computed from the Rf between the analytes and the IS (fluoranthene). Other compounds, not listed above, were calculated by regarding as 1.0.

3. Results and discussion

3.1 Catalyst characteristics

3.1.1 Morphology of carbon supports and textural properties of the supported catalysts

Figure 2 shows the FE-SEM images of carbon support structures (C, STC, TC, and DC). It can be seen that the carbon particles in Pt/C are spherical in shape with small pores in between the carbon agglomerates. The surface is rough, indicating uniformly-developed porosity. Likewise, the DC, TC, and STC supports showed well-developed porosity with rough surfaces. However, the DC support showed narrow and slit pores, which makes it more difficult to distinguish the boundary between the DC support and the Pt catalyst. Alternatively, the TC and STC supports showed more complex and rough surfaces compared to the DC support. In contrast to the C support, STC exhibited non-spherical, entangled carbon structures; this had the most complex and interconnected pore structure. According to the above results, the STC support is considered to be the best support material in terms of its porous structure.

The textural properties of the supported catalysts (Pt/C, Pt/STC, Pt/TC, and Pt/DC) are summarized in Table 1. This table includes the BET surface area, pore volume, average pore size, and micropore area. The obtained BET surface areas show that Pt/STC had a relatively higher surface area (832.62 m^2/g) compared to Pt/TC and Pt/DC (490.93 m^2/g and 374.35 m^2/g, respectively). This suggests that the Pt particles are well-distributed on the STC support structures. However, when compared to the commercial catalyst, Pt/STC was only 55% of the value of Pt/C (1506.49 m^2/g). This reveals the challenges that remain to be solved when manufacturing sophisticated arrays of Pt particles on carbon supports. Pore volumes of the Pt/C and PT/STC catalysts were 1.25 cm^3/g and 1.06 cm^3/g, respectively, while the Pt/TC and Pt/DC supports exhibited negligible pore volumes. Additionally, the average pore sizes were in the sequence of Pt/STC (44.82 A) > Pt/C (43.14 A) > Pt/TC (40.03 A) > Pt/DC (32.71 A) as shown in Figure S1. However, the Pt/DC catalyst had a large micropore area (505 m^2/g-cat.) due to the well-developed micropores of the DC support.

3.1.2 Crystalline phase and platinum dispersion on carbon-supported catalysts

The Pt nanoparticles supported on C, STC, TC, and DC exhibit X-ray diffraction patterns of a typical face-centered-cubic (fcc) lattice structure, as shown in Figure 3. The strong diffraction peaks at Bragg angles of 39.76, 46.24, 67.45, and 81.28 (2 Theta) correspond to the (111), (200), (220), and (311) facets of a Pt crystal, respectively, demonstrating the presence of Pt in a metallic form [20]. It was observed that the Pt peak intensity of Pt on carbon supports decreased in the order of Pt/DC > Pt/TC > Pt/STC > Pt/C, indicating that Pt particles were most finely dispersed on the C supports [18(a)]. In addition, the Pt (111) peak was used to calculate the particle size of Pt (according to the Scherrer equation). The Pt nanoparticle sizes of Pt/C, Pt/STC, Pt/TC, and Pt/DC were 3.5, 5.3, 10.3, and 21.8 nm, respectively. It is expected that the increased dispersion of Pt particles supported on carbon, with smaller particle sizes, should result in an increase in the active area and enable better catalytic performance. Since the sizes of Pt particles are apparently different as shown above, the property of Pt particles on each support may differ as well. Therefore, X-ray photoelectron spectra (XPS) has been used to obtain information about interaction of Pt particles with carbon supports and their relative intensities. Figure S2 shows the result of Pt 4f electron signals. In XPS studies, the Pt 4f signal has always provided the valuable information [21]. As shown in spectra, all the catalysts are well resolved with two doublets except Pt/STC. The most intense ones, located around 71.1 and 75.6 eV, are due to metallic Pt (Pt $4f_{7/2}$ and Pt $4f_{5/2}$) and these peaks are affected by the interactions between Pt and C [22]. The Pt binding energy in Pt/C, Pt/STC, Pt/TC and Pt/DC is varied from 71.4 to 76.1 eV, respectively, indicating that there is a shift of 0.3-0.5 eV compared to the binding energies of bulk Pt, and this further shift was probably attributed to stronger Pt-support interactions or small particle effect [23]. This Pt-carbon support interaction is considered to be beneficial to the enhancement of catalytic properties and to improve stability of the electrocatalyst. Furthermore, the line at

lower binding energies shown in spectra is undoubtedly due to Pt(0), while the line at higher binding energy component is due to PtO_2 or $Pt(OH)_4$ and the relative intensities of the Pt(0), PtO_2 or $Pt(OH)_4$ are summarized in Table S2. The results gives that metallic Pt(0) is the major species in all the catalysts (>70%) with a smaller amount of an oxidized Pt species (<30%). It is believed that catalysts with Pt(0) is more effective in providing active site for depolymerization reaction rather than PtO_2 or $Pt(OH)_4$ [24-26]. Therefore, to obtain high catalytic activity for these Pt based catalysts, having a large amount of metallic Pt(0) is required. These differences in property of Pt particles on each catalyst will significantly involve in catalytic performance. For example, the catalytic activity of the dispersed metals on the supports is influenced by many factors such as the relative amount of metals present, extent of dispersion, chemical nature of the support, and strength of interaction between the support and the metal [27-31]. When comparing only the catalysts that were prepared in our laboratory (i.e., Pt/STC, Pt/TC, and Pt/DC but excluding the commercial catalyst (Pt/C)), the Pt peak intensity of the Pt/STC catalyst was smaller than that of Pt/TC and Pt/DC; this indicates that the metal may be aggregated in small clusters with finely dispersed structures, resulting in high catalytic activity [32]. This result is caused by the structure of STC, which consists of well-developed pores created by the use of a surfactant [18(a)].

Figure 4 shows the HR-TEM images of the Pt/C, Pt/STC, Pt/TC, and Pt/DC samples reduced at 300 °C. As shown in the image, the Pt particles on the mesoporous catalysts (C, STC, and TC) are uniform and well-distributed. Additionally, it can be seen that very few catalyst particles are agglomerated. Alternatively, the microporous catalyst (Pt/DC) retained Pt particle aggregates; therefore, it was difficult to see the structure of the Pt particles dispersed on the DC support. In particular, Pt particles on the C and STC supports were not only more finely dispersed but their arrayed patterns were also more constantly arranged compared to those of the TC or DC supports. This result indicates that the pore volume of the

carbon support plays a significant role in terms of increasing the Pt dispersion on the carbon supports. The different pore volumes are believed to be due to the different surface chemistries of the carbon supports [33].

3.2 Catalytic degradation of lignin

3.2.1 Yield of depolymerized lignin products

Depolymerization of the soda lignin over the different supported catalysts (Pt/C, Pt/STC, Pt/TC, and Pt/DC) was performed at 350 °C for 40 min under 3 MPa of hydrogen. It was found that the decomposition of lignin generated three main products: an aqueous phenolic compounds fraction (lignin-oil), char, and gas. The lignin-oil yield ranged from 54.4 wt% to 82.5 wt%, depending on the different supported catalysts; these yields were slightly higher than the results of previous studies (33 to 78 wt%) [34].

This lignin-oil contains high amounts of aromatics and alkylphenolics. Alternatively, the formation of low-value side residues (gas and char) during the side reactions (recondensation, carbonization, and further decomposition) was later observed to inhibit the production of monomeric phenols. In order to prevent these undesired reactions, the selection of a catalyst that reduces side reactions while also specializing in hydrogenation or hydro-deoxygenation reactions is considered to be an important factor.

The lignin-oil, char, and gas yields over the different carbon-supported Pt catalysts are presented in Figure 5. These results show that applying mesoporous catalysts (Pt/C, Pt/STC, and Pt/TC) in the lignin depolymerization process leads to an increase in the production of both lignin-oil and gas while the char formation is decreased. Alternatively, the microporous (Pt/DC) catalyst had a large amount of char with a low yield of lignin-oil. This indicates, as mentioned above, that the pore volume of the carbon support plays an important role in increasing the Pt dispersion on the carbon support, which subsequently enhances the

conversion reaction of lignin into lignin-oil. In addition, due to the agglomerated Pt particles distributed on the DC (as shown in HR-TEM result), the catalytic reaction was not efficiently progressed. When viewed in terms of the highest yield of lignin-oil and the smallest amount of char, Pt/C (79.9 wt% and 4.2 wt%, respectively) and Pt/STC (79.4 and 7.6 wt%, respectively) proved to be excellent catalysts for lignin depolymerization.

3.2.2 Chemical properties of lignin-oil

As reported in many previous studies, lignin-oil that has been depolymerized over noble metal catalysts has the potential to be used as a renewable starting material for the production of high value-added chemicals. However, the exact chemical composition of the lignin-oil is often not given. In this study, changes in the chemical properties of lignin-oil as a function of the different supported catalysts were analyzed by GPC and elemental analysis.

Table 2 shows the average molecular weights (M*w* and Mn), polydispersity indices (PDI: M*w*/Mn), and elemental compositions of the catalytically depolymerized lignin-oil. The molecular weights of lignin-oil ranged from 600 Da (for Pt/C: 601 Da and Pt/STC: 674 Da) to 700 Da (for Pt/TC: 738 Da and Pt/DC: 745 Da), which were only 16 to 21% of the molecular weight of soda lignin (3,698 Da). This demonstrates that all of the carbon-supported Pt catalysts effectively underwent lignin decomposition during the depolymerization process. Moreover, the polydispersity index also decreased from 2.68 (soda lignin) to 1.4 for Pt/C, 1.6 for Pt/STC, and 1.8 for Pt/TC and Pt/DC, which proves that the size of the lignin fragments (consisting of lignin-oil) is uniformly-dispersed compared to soda lignin.

The elemental compositions (C, H, N, S, and O) of the lignin-oil were determined and are shown in Table 2. Applying carbon-supported Pt catalysts to lignin depolymerization yielded low molecular weights and hydro-deoxygenated lignin oils with O/C ratios that were

significantly lower than the starting lignin. Compared to the carbon and oxygen contents of soda lignin, the carbon contents of lignin-oil were increased to 70.1% for both Pt/C and Pt/STC, 69.2% for Pt/TC, and 68.3% for Pt/DC. The oxygen contents were decreased to 21.2% for Pt/C, 21.4% for Pt/STC, 22.5% for Pt/TC, and 23.6% for Pt/DC. These results are due to the fact that Pt/C is known to be a hydro-deoxygenation catalyst and is expected to decrease the O/C molar ratios [35].

3.2.3 Yield of monomeric phenols in lignin-oil

Table 3 illustrates the GC-detectable compounds in lignin-oils. The reaction generated 4-ethylphenol, 4-methylguaiacol, 4-ethylguaiacol, and 4-propylguaiacol as the major products. The minor products were aliphatic fatty acid ester or ethyl ester. These alkyl phenolics likely arise from lignin depolymerization over the catalytic hydrogenation or hydro-deoxygenation reactions [36]. These phenol products have significant potential as a source for the sustainable production of fuels and bulk chemicals [37], as well as a variety of products including insulation materials, rubber, lacquers, paint, adhesives, ink, dyes, illuminating gases, perfumes, medicine, and soaps.

In particular, Pt/C shows the highest abundance of highly hydrogenated compounds and a lower amount of oxygenated compounds (90.92 mg/g of lignin). This is followed by Pt/STC (78.06 mg/g of lignin), Pt/TC (64.33 mg/g of lignin), and Pt/DC (53.22 mg/g of lignin). As shown above in 3.3.1, the main disadvantage of the Pt/DC catalyst is the extensive repolymerization of the lignin into char; this char adheres to the surface of the catalyst, deactivating the catalyst reaction. Due to this obstacle, Pt/DC had the lowest yield of monomeric phenols and does not provide a significantly greater amount of the desired compound. However, both the major products and the total yields were improved for Pt/C and Pt/STC, as compared to Pt/TC and Pt/DC. This indicates that when the Pt particles are

more finely dispersed on the carbon supports, the degradation of lignin into monomeric phenols is improved.

3.3 Correlation between catalyst surface areas and the lignin-oil properties

In this study, the relationship between the BET surface areas of the carbon-supported Pt catalysts (Pt dispersion) and the catalytic activity in the depolymerization of lignin into monomeric phenols is established. The correlations between the BET surface areas of Pt/C, Pt/STC, Pt/TC, and Pt/DC catalysts and the effects of the catalytic activity in the molecular characteristics of lignin-oil as well as the amount of monomeric phenols in the lignin-oil are shown in Figures 6 and 7, respectively. As the BET surface area of the carbon-supported Pt catalysts increases, the molecular weight of the lignin-oil is reduced and the PDI decreases. This indicates that catalysts with a higher surface area lead to effective depolymerization and more uniformly sized lignin fragments in the lignin-oil. Although the yields of the major products (4-ethylphenol, 4-methylguaiacol, 4-ethylguaiacol, and 4-propylguaiacol) are affected by the additional decomposition and recondensation reactions that occur during lignin depolymerization (i.e., the formation of char), the total yield for monomeric phenols still increases with increasing BET surface area. Hong et al. have studied the hydrogenation of succinic acid into γ-butyrolactone over ruthenium catalysts supported on surfactant-templated carbon. They showed that a more finely-dispersed catalyst (i.e., a higher catalyst surface area) leads to a higher yield of the hydrogenation product with higher selectivity [18(a)]. Accordingly, the BET surface area of carbon-supported Pt catalysts plays an important role for effective depolymerization and conversion of lignin into monomeric phenols.

4. Conclusions

We established correlations between the catalyst surface area and the characteristics of the depolymerized lignin products. Surface area of the catalyst was in the order of Pt/C (1506.49 m^2/g-cat.) > Pt/STC (832.62 m^2/g-cat.) > Pt/TC (490.93 m^2/g-cat.) > Pt/DC (374.35 m^2/g-cat.). Yield of the low molecular weight lignin-oil and the yield of the monomeric phenols followed the same trend as the BET surface area. In particular, Pt/STC produced lignin-oil with the lowest molecular weight (674 Da) and a higher degree of conversion into monomeric phenols (78.06 mg/g of lignin) compared to Pt/TC or Pt/DC. This excellent catalyst reaction was due to the fine dispersion of Pt particles on the STC support (i.e., high BET surface area).

Acknowledgements

This research was supported by Basic Science Research Program through the National Research Foundation (NRF), funded by the Ministry of Education, Science and Technology (Project No. 2013R1A2A2A01011112).

Reference

1. G. Brunow, K. Lundquist, in *Functional groups and bonding patterns in lignin (including the lignin-carbohydrate complexes)*, CRC Press, Taylor Francis Group, New York, 2010, pp. 272-281.
2. E. Gnansounou, A. Dauriat, *Bioresour. Technol.,* 2010, 101, 4980-4991.
3. S. Farag, L. Kouisni, J. Chaouki, *Energy Fuels,* 2014, 28, 1406-1417.
4. S. K. Singh, J. D. Ekhe, *Catal. Sci. Technol.,* 2015, 5, 2117-2124.
5. (a) J. Das, A. B. Halgeri, *Appl.Catal. A,* 2000, 194, 359-363; (b) M. Sasaki, M. Goto, *Chem. Eng. Process.,* 2008, 47, 1609-1619.
6. J. Miller, L. Evans, A. Littlewolf, D. Trudell, *Fuel,* 1999, 78, 1363-1366.
7. (a) Q. Song, F. Wang, J. Cai, Y. Wang, J. Zhang, W. Yu, J. Xu, *Energ. Environ. Sci.* 2013, 6, 994-1007; (b) V. Roberts, V. Stein, T. Reiner, A. Lemonidou, X. Li, J. A. Lercher, *Chem. Eur. J.,* 2011, 17, 5939-5948.
8. (a) J. Gagnon, S. Kaliaguine, *Ind. Eng. Chem. Res.,* 1988, 27, 1783-1788; (b) Y.-H. E. Sheu, R. G. Anthony, E. J. Soltes, *Fuel Process. Technol.,* 1988, 19, 31-50; (c) D. C. Elliott, K. L. Peterson, D. S. Muzatko, E. V. Alderson, T. R. Hart, G. G. Neuenschwander, in *Proceedings of the Twenty-Fifth Symposium on Biotechnology for Fuels and Chemicals Held May 4–7, 2003, in Breckenridge, CO*, Springer, 2004, pp. 807-825.
9. T. Marzialetti, S. J. Miller, C. W. Jones, P. K. Agrawal, *J. Chem. Technol. Biotechnol.,* 2011, 86, 706-713.
10. N. Yan, C. Zhao, P. J. Dyson, C. Wang, L. t. Liu, Y. Kou, *ChemSusChem,* 2008, 1, 626-629.
11. J.-Y. Kim, J. Park, U.-J. Kim, J. W. Choi, *Energy Fuels,* 2015, 29, 5154-5163.
12. N. Yan and X. Chen, *Nature*, 2015, **524**, 155-157.
13. P. H. Matter, L. Zhang and U. S. Ozkan, *Journal of Catalysis*, 2006, **239**, 83-96.
14. T. Maiyalagan, B. Viswanathan and U. Varadaraju, *Electrochemistry Communications*, 2005, **7**, 905-912.
15. Y. Gao, X. Chen, J. Zhang and N. Yan, *ChemPlusChem*, 2015, **80**, 1556-1564.
16. (a) J.-Y. Miao, D. W. Hwang, C.-C. Chang, S.-H. Lin, K. Narasimhulu, L.-P. Hwang, *Diam. Relat. Mater.,* 2003, 12, 1368-1372; (b) Q. Wang, H. Li, L. Chen, X. Huang, *Carbon,* 2001, 39, 2211-2214.
17. E. P. Ambrosio, C. Francia, M. Manzoli, N. Penazzi, P. Spinelli, *Int. J. Hydrogen Energ.,* 2008, 33, 3142-3145.
18. (a) U. G. Hong, H. W. Park, J. Lee, S. Hwang, I. K. Song, *J. Ind. Eng. Chem.* 2012, 18, 462-468; (b) J. Zakzeski, A. L. Jongerius, P. C. Bruijnincx, B. M. Weckhuysen, *ChemSusChem,* 2012, 5, 1602-1609.
19. J.-Y. Kim, S. Oh, H. Hwang, T.-s. Cho, I.-G. Choi, J. W. Choi, *Chemosphere,* 2013, 93, 1755-1764.
20. F. Su, J. Zeng, X. Bao, Y. Yu, J. Y. Lee, X. Zhao, *Chem. Mater.,* 2005, 17, 3960-3967.
21. F. Coloma, A. Sepúlveda-Escribano, J. Fierro and F. Rodriguez-Reinoso, *Applied Catalysis A: General*, 1996, **148**, 63-80.
22. Z. Q. Tian, S. P. Jiang, Y. M. Liang and P. K. Shen, *The Journal of Physical Chemistry B*, 2006, **110**, 5343-5350.
23. J. B. Goodenough, R. Manoharan, A. Shukla and K. Ramesh, *Chemistry of Materials*, 1989, **1**, 391-398.
24. P.-L. Kuo, W.-F. Chen, H.-Y. Huang, I.-C. Chang and S. A. Dai, *The Journal of Physical Chemistry B*, 2006, **110**, 3071-3077.

25. J. Goodenough, A. Hamnett, B. Kennedy, R. Manoharan and S. Weeks, *Journal of electroanalytical chemistry and interfacial electrochemistry*, 1988, **240**, 133-145.
26. M. Watanabe, M. Uchida and S. Motoo, *Journal of electroanalytical chemistry and interfacial electrochemistry*, 1987, **229**, 395-406.
27. E. Antolini, *Applied Catalysis B: Environmental*, 2009, **88**, 1-24.
28. M. L. Toebes, J. A. van Dillen and K. P. de Jong, *Journal of Molecular Catalysis A: Chemical*, 2001, **173**, 75-98.
29. G. C. Bond, *Metal-catalysed reactions of hydrocarbons*, Springer, 2005.
30. R. Downing, P. Kunkeler and H. Van Bekkum, *Catalysis Today*, 1997, **37**, 121-136.
31. L. Okhlopkova, A. Lisitsyn, V. Likholobov, M. Gurrath and H. Boehm, *Applied Catalysis A: General*, 2000, **204**, 229-240.
32. D. K. Liguras, D. I. Kondarides, X. E. Verykios, *Appl. Catal. B,* 2003, 43, 345-354.
33. K.-Y. Chan, J. Ding, J. Ren, S. Cheng, K. Y. Tsang, *J. Mater. Chem.* 2004, 14, 505-516.
34. (a) J. A. Onwudili, P. T. Williams, *Green Chem.,* 2014, 16, 4740-4748; (b) X. Huang, T. I. Korányi, M. D. Boot, E. J. Hensen, *ChemSusChem,* 2014, *7*, 2276-2288; (c) K. Barta, G. R. Warner, E. S. Beach, P. T. Anastas, *Green Chem.,* 2014, 16, 191-196; (d) A. Kloekhorst, H. J. Heeres, *ACS Sustainable Chem. Eng.* 2015, 3, 1905-1914.
35. X. Xu, Y. Li, Y. Gong, P. Zhang, H. Li, Y. Wang, *J. Am. Chem. Soc.,* 2012, 134, 16987-16990.
36. A. Kloekhorst, Y. Shen, Y. Yie, M. Fang, H. J. Heeres, *Biomass Bioenerg.,* 2015, 80, 147-161.
37. (a) R. D. Perlack, *et al.*, *Biomass as Feedstock for a Bioenergy and Bioproducts Industry: The Technical Feasibility of a Billion-Ton Annual Supply*, U.S. Department of Energy and U.S. Department of Agriculture, 2005; (b) T. Werpy, G. Petersen, A. Aden, J. Bozell, J. Holladay, J. White, A. Manheim, D. Eliot, L. Lasure and S. Jones, *Top Value Added Chemicals from Biomass. Volume 1-Results of Screening for Potential Candidates from Sugars and Synthesis Gas*, DTIC Document, 2004

Figure captions

Figure 1. Schematic procedures for the preparation of carbon supports

Figure 2. FE-SEM images of (a) Pt/DC (b) Pt/TC (c) Pt/STC and (d) Pt/C

Figure 3. XRD patterns of carbon supported Pt catalysts

Figure 4. HR-TEM images of carbon supported Pt catalysts

Figure 5. The yields of lignin depolymerized products

Figure 6. Correlations between BET surface area of carbon supported Pt catalysts and the molecular characteristics of lignin-oil ■molecular weight (Da); ◇polydispersity index

Figure 7. Correlations between BET surface area of carbon supported Pt catalysts and the amount of monomeric phenols in the lignin-oil

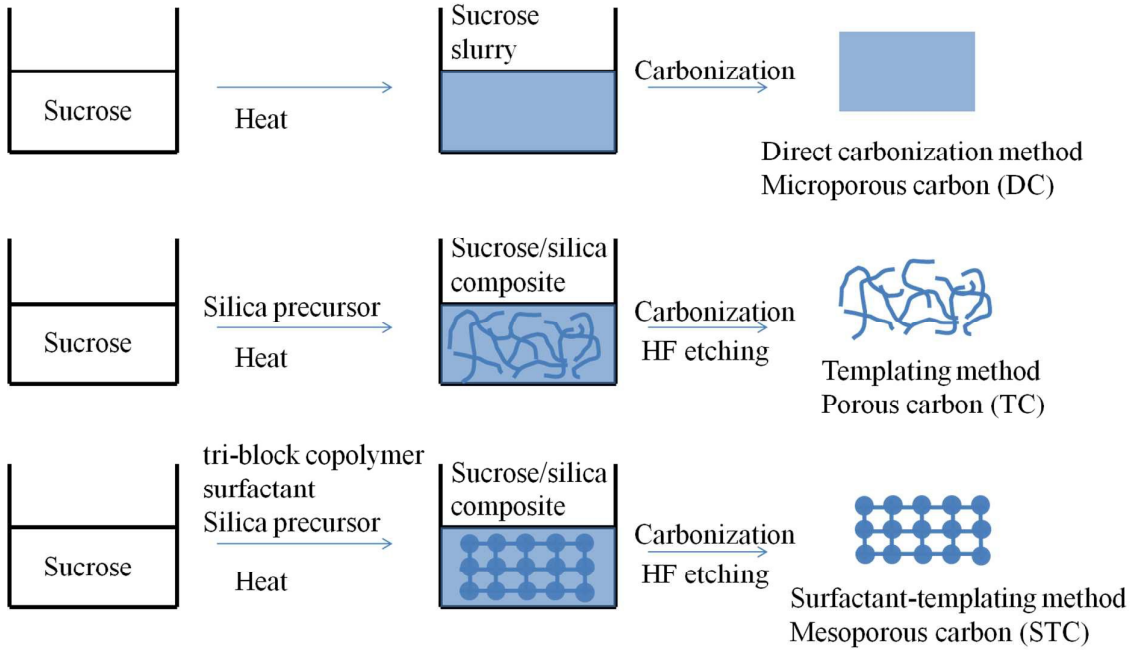

Figure 1. Schematic procedures for the preparation of carbon supports [14(a)]

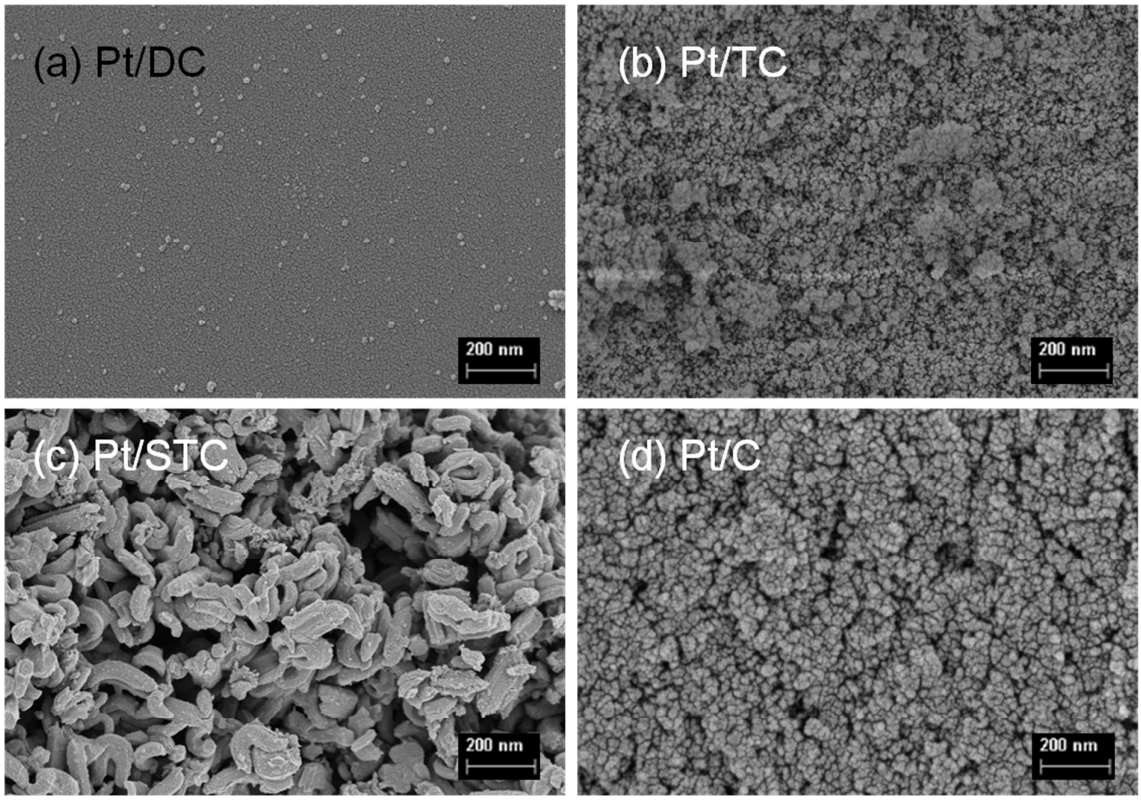

Figure 2. FE-SEM images of (a) Pt/DC (b) Pt/TC (c) Pt/STC and (d) Pt/C

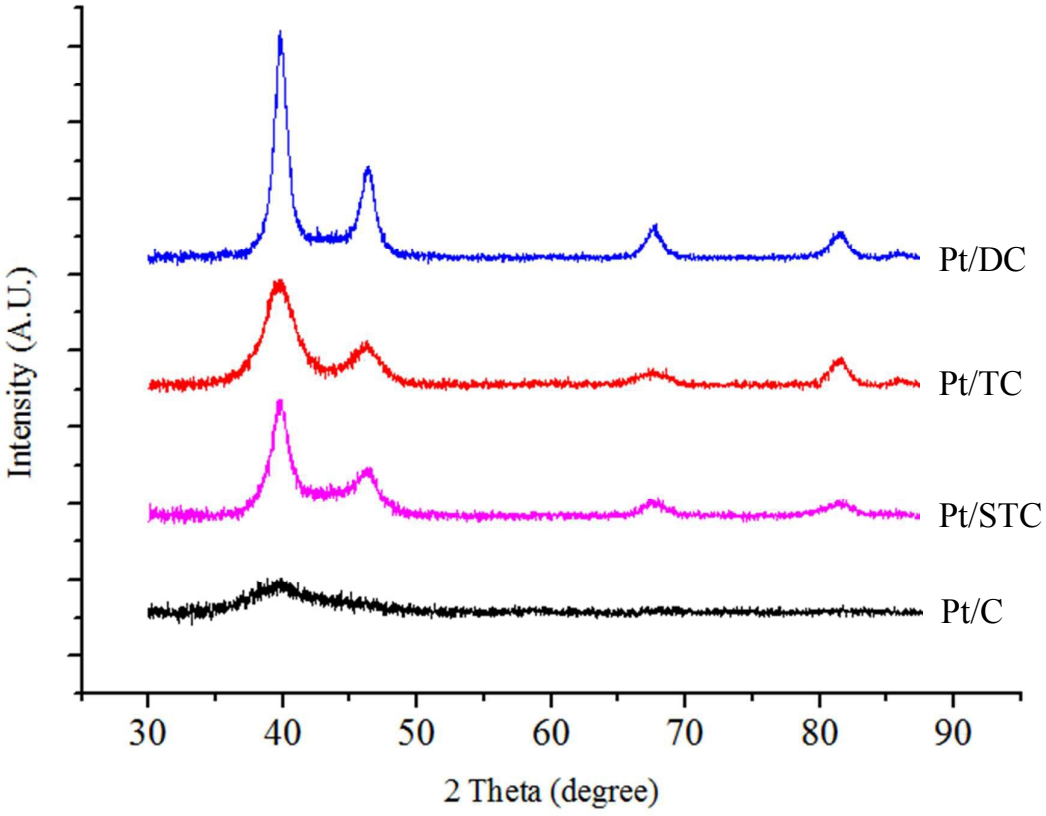

Figure 3. Comparison of XRD patterns obtained from various carbon supported Pt catalysts

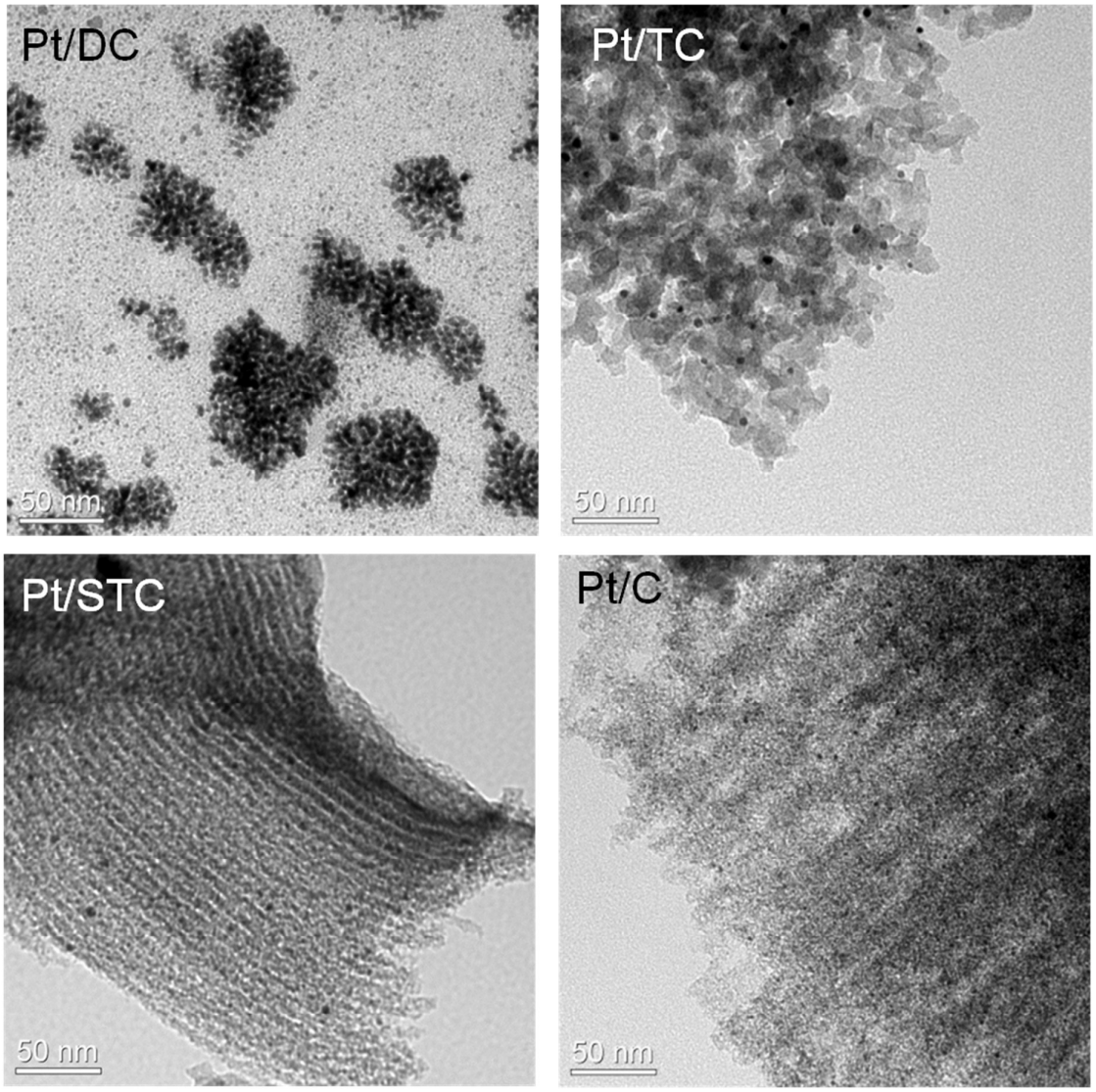

Figure 4. HR-TEM images of various carbon supported Pt catalysts

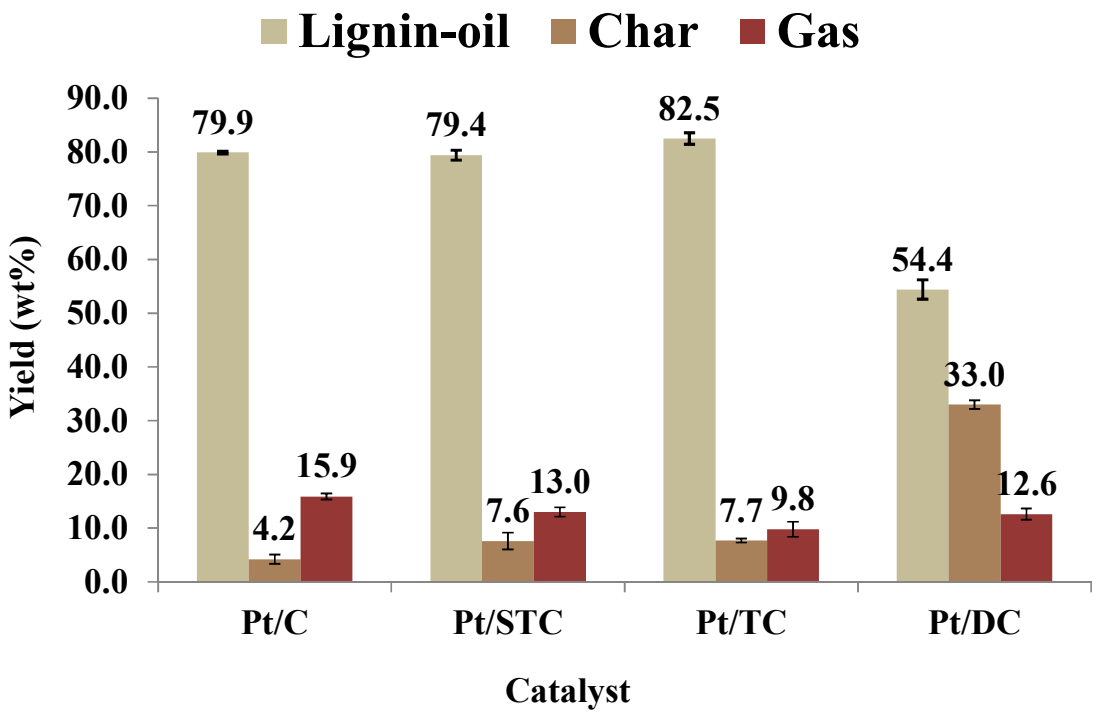

Figure 5. The mass balance of lignin depolymerized products in the presence of Pt-catalysts prepared with carbon supports.

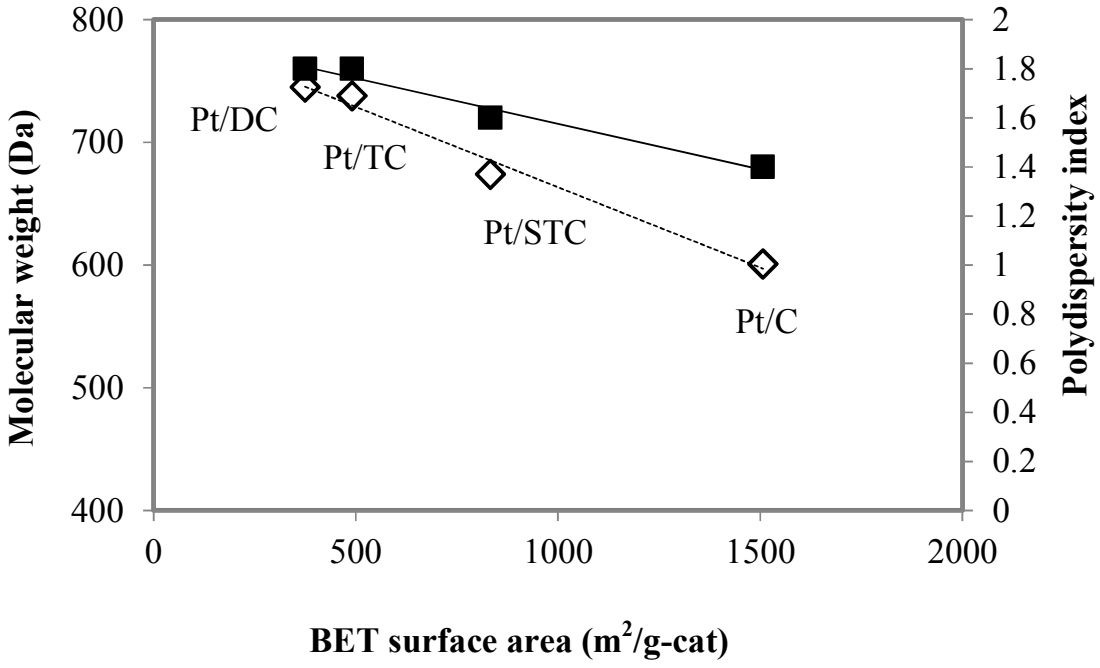

Figure 6. Correlations between BET surface area of carbon supported Pt catalysts and th e molecular characteristics of lignin-oil ■molecular weight (Da); ◇polydispersity index

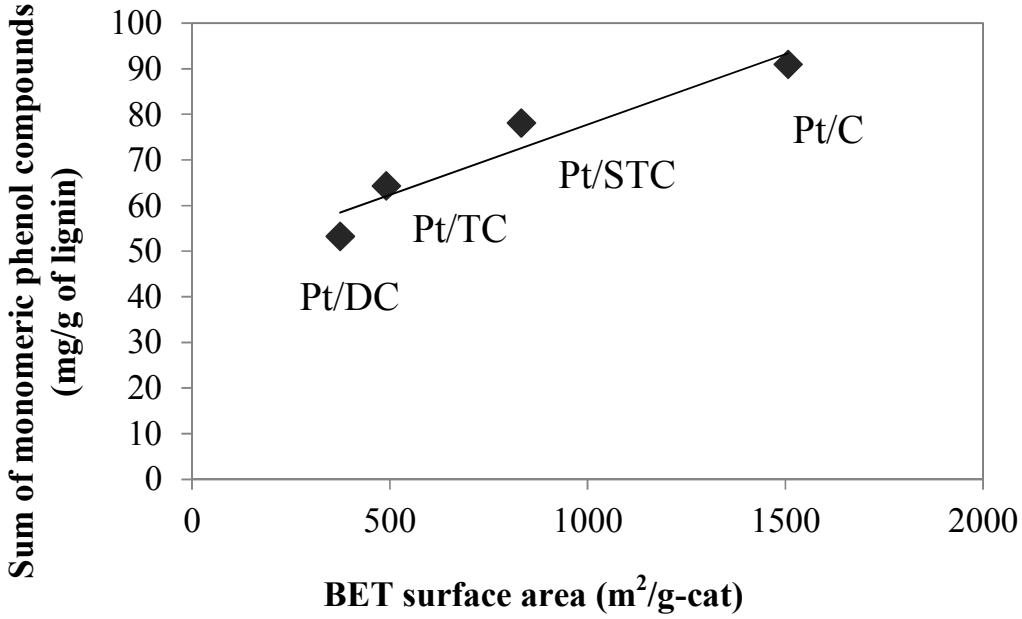

Figure 7. Correlations between BET surface area of carbon supported Pt catalysts and the amount of monomeric phenols in the lignin-oil

Table captions

Table 1. Textural properties of carbon supported Pt catalysts.

Table 2. The elemental compositions and the average molecular weights (M*w* and Mn) with polydispersity indexes (M*w*/Mn) of the oils

Table 3. The amount of monomeric phenols in lignin-oil over carbon supported Pt catalysts

Table 1. Textural properties of carbon supported Pt catalysts.

Sample	BET surface area (m^2/g-cat.)	Pore volume (cm^3/g-cat.)	Average pore size (A)	Micropore area (m^2/g-cat.)
Pt-C	1506.49	1.25	43.14	292
Pt-DC	374.35	-	32.71	505
Pt-TC	490.93	-	40.03	120
Pt-STC	832.62	1.06	44.82	284

Table 2. The elemental compositions and the average molecular weights (M*w* and Mn) with polydispersity indexes (M*w*/Mn) of the oils

Sample	Elemental composition (%)					*M*w (Da)	*M*n (Da)	PDI (*M*w/*M*n)
	C	H	N	S	O[a]			
PT-C	70.1	7.4	0.8	0.5	21.2	601	415	1.4
PT-DC	68.3	7.0	0.6	0.5	23.6	745	417	1.8
PT-TC	69.2	7.1	0.7	0.5	22.5	738	400	1.8
PT-STC	70.1	7.2	0.8	0.5	21.4	674	410	1.6

[a] Calculated by difference

Table 3. The amount of monomeric phenols in lignin-oil over carbon supported Pt catalysts

Peak No.	Compounds	Yield of monomeric phenols (mg/g of lignin)								
		RT[a]	PT-C	SD[b]	PT-STC	SD	PT-TC	SD	PT-DC	SD
1	Phenol	15.24	1.42	0.2	2.28	0.3	1.48	0.5	2.62	0.4
2	o-cresol	19.00	0.52	0.0	0.13	0.0	0.40	0.0	0.63	0.1
3	p-cresol	20.14	1.88	0.2	1.56	-	1.85	0.3	2.09	0.2
4	Guaiacol	20.72	5.70	0.6	5.45	0.5	2.72	0.8	4.76	0.4
5	2-Ethylphenol	23.15	0.83	0.1	0.42	0.1	0.70	0.1	0.82	0.2
6	2,4-Dimethylphenol	23.72	-	-	0.19	-	0.42	0.1	0.25	0.1
7	4-Ethlyphenol	24.68	9.86	0.4	8.73	-	9.58	1.0	9.22	0.3
8	3-Methylguaiacol	25.12	0.46	0.1	0.32	-	-	-	-	-
9	4-Methylguaiacol	25.81	5.87	0.2	6.08	-	-	-	-	-
10	Benzofuran	27.11	0.5	0.2	0.10	0.8	7.19	3.0	1.30	0.5
11	2-Ethyl-5-methylphenol	27.98	0.13	0.4	0.52	-	-	-	-	-
12	3-Methoxycathecol	28.83	1.04	0.5	2.84	0.7	0.77	0.1	0.83	0.1
13	4-Ethylguaiacol	29.82	5.29	0.2	10.64	-	0.80	0.3	1.51	0.0
14	4-Vinylguaiacol	31.34	8.30	0.4	0.58	0.1	6.44	1.2	1.78	0.6
15	4-ethyl-1,2-dimethoxybenzene	31.80	3.27	0.2	0.57	-	1.67	0.2	2.55	0.3
16	Syringol	33.04	4.24	0.4	6.26	0.1	3.69	0.5	4.22	1.2
17	4-Propylguaiacol	33.68	10.41	0.5	4.19	-	3.72	0.5	4.28	1.1
18	4-Methylsyringol	37.03	0.84	0.7	4.06	0.3	5.48	1.6	4.73	1.9
19	trans-isoeugenol	37.26	-	-	5.71	0.4	2.08	0.6	3.57	0.1
20	Acetoguaiacone	38.67	3.63	0.8	0.42	0.2	5.06	2.1	3.33	1.4
21	4-Ethylsyringol	40.15	0.72	0.6	4.30	-	-	-	-	-
22	Guaiacyl acetone	40.32	0.19	0.6	0.42	0.4	4.76	1.3	2.15	0.6
23	Homovanillyl alcohol	40.41	10.75	0.4	0.25	0.2	2.52	0.7	0.29	0.1
24	Vanillic acid, ethyl ester	42.62	1.08	0.2	0.30	-	-	-	-	-
25	4-Propylsyringol	43.39	-	-	3.43	-	1.68	0.7	0.36	0.0
26	Ethyl homovanillate	44.61	1.12	0.1	0.56	-	-	-	-	-
27	Acetosyringone	47.94	-	-	5.87	-	0.43	0.1	1.22	0.5
28	4-Hydroxy-3-Methoxybenzenpropanoic acid, ethyl ester	48.51	12.09	0.4	1.21	-	-	-	-	-
29	Palmitic acid, ethyl ester	56.84	0.78	0.1	0.67	-	0.89	0.1	0.71	0.2
	Sum of phenol compounds		90.92		78.06		64.33		53.22	

[a] RT represents retention time in minute
[b] SD stands for standard deviation

Graphical abstract